Capicua regulates proliferation and survival of RB-deficient cells in *Drosophila*

Kate Krivy, Mary-Rose Bradley-Gill and Nam-Sung Moon*

Department of Biology, Developmental Biology Research Initiative, McGill University, Montreal, QC H3A 1B1, Canada

*Author for correspondence (nam.moon@mcgill.ca)

Biology Open 2, 183–190
doi: 10.1242/bio.20123277
Received 9th October 2012
Accepted 1st November 2012

Summary

Mutations in *rbf1*, the *Drosophila* homologue of the *RB* tumour suppressor gene, generate defects in cell cycle control, cell death, and differentiation during development. Previous studies have established that EGFR/Ras activity is an important determinant of proliferation and survival in *rbf1* mutant cells. Here, we report that Capicua (Cic), an HMG box transcription factor whose activity is regulated by the EGFR/Ras pathway, regulates both proliferation and survival of RB-deficient cells in *Drosophila*. We demonstrate that *cic* mutations allow *rbf1* mutant cells to bypass developmentally controlled cell cycle arrest and apoptotic pressure. The cooperative effect between Cic and RBF1 in promoting G1 arrest is mediated, at least in part, by limiting Cyclin E expression. Surprisingly, we also found evidence to suggest that *cic* mutant cells have decreased levels of reactive oxygen species (ROS), and that the survival of *rbf1* mutant cells is affected by changes in ROS levels. Collectively, our results elucidate the importance of the crosstalk between EGFR/Ras and RBF1 in coordinating cell cycle progression and survival.

Key words: *rbf1*, RB, *Capicua*, Cell cycle regulation, Eye development

Introduction

The product of the Retinoblastoma tumour suppressor gene *RB* acts to control the cell cycle, cell death and differentiation during development (Sherr, 1996; Stevaux and Dyson, 2002; van den Heuvel and Dyson, 2008). Thus, loss of RB function, a frequent event in cancer, can lead to defects in various biological processes. A large fraction of these defects are believed to be mediated via the E2F family of transcription factors (Dimova and Dyson, 2005; Dyson, 1998). In quiescent cells, RB family proteins bind to E2F transcription factors, facilitating repression of genes that are necessary for the transition into the S phase of the cell cycle. When RB becomes hyperphosphorylated by Cyclin Dependent Kinases (CDK), interaction with E2Fs is inhibited, and, as a consequence, E2Fs proceed to activate genes involved in the progression of the cell cycle. Accordingly, in cancers, E2F transcription factors are constitutively active resulting in a lack of cell cycle control and uncontrolled proliferation.

While it is clear that E2F transcription factors play a central role, accumulating evidence suggests that there are secondary factors that facilitate development of RB-deficient cancers. Careful analysis of tissue samples from retinoblastoma patients has revealed that an increase in genomic instability correlates with a progression from non-proliferative retinomas to aggressive retinoblastomas (Bowles et al., 2007). Furthermore, inactivation of CDH11, one of the genes that is frequently lost in retinoblastoma, has been shown to promote survival of tumours in a Large T-antigen-induced mouse retinoblastoma model (Marchong et al., 2010). In a more recent study, integrative analysis of epigenomics and gene expression profiles identified that the expression of Spleen Tyrosine Kinase (SYK) is deregulated in retinoblastoma and has proven to be a potential therapeutic target (Zhang et al., 2012). Taken together, these studies indicate that factors other than E2Fs are deregulated in retinoblastoma and contribute to the tumorigenesis of RB-deficient cancer. Evidently, identification of such factors and elucidation of their molecular mechanisms can help us to better understand and target cancer cells.

Drosophila melanogaster provides a context in which the composition of RB/E2F family proteins is simplified, while the biological function is highly conserved. (Stevaux and Dyson, 2002; van den Heuvel and Dyson, 2008). RBF1 is the functional homologue of the RB tumour suppressor protein that regulates the two E2F transcription factors, dE2F1 and dE2F2. dE2F1 behaves as an activator while dE2F2 behaves as a repressor of transcription. This is in contrast to the complex mammalian system, composed of eight E2F proteins and two additional RB family proteins, p107 and p130, which have redundant function to RB. The simplified context of *Drosophila* RB/E2F provides a convenient genetic system to study their biological function during development.

In the *Drosophila* eye, RBF1 cooperates with the EGFR/Ras pathway to protect cells entering the morphogenetic furrow (MF) from apoptosis and to maintain cell cycle arrest of differentiating photoreceptors (Firth and Baker, 2005; Moon et al., 2006). At the molecular level, transcription of the pro-apoptotic gene *hid* is controlled by RBF1 while the activity of the gene product is regulated by the EGFR/Ras pathway via phosphorylation (Bergmann et al., 1998; Kurada and White, 1998; Moon et al., 2006; Moon et al., 2005). Moreover, expression of Dacapo (Dap), the *Drosophila* homologue of p21/27, accumulates in response to

EGFR/Ras signalling (Firth and Baker, 2005). The primary function of Dap is to antagonize CDK2 whose kinase activity requires Cyclin E, a well-known transcriptional target of RBF1. As a consequence, at least in the context of eye development, the EGFR/Ras pathway is an important determinant of proliferation and survival of RB-deficient cells in *Drosophila*.

In an effort to comprehend the crosstalk that exists between RBF1 and the EGFR/Ras pathway, Capicua (Cic) emerged as a candidate protein that might cooperate with RBF1 to regulate proliferation. Cic is an HMG box transcription factor and was first identified as being essential for the establishment of dorsal–ventral polarity of the *Drosophila* egg (Jiménez et al., 2012). In this process, the EGFR/Ras pathway post-transcriptionally regulates Cic expression through a MAPK docking site at the C-terminus of Cic (Astigarraga et al., 2007). Notably, in the developing *Drosophila* eye, Cic is shown to restrict the rate of proliferation in response to EGFR/Ras activity, and the loss of Cic bypasses the requirement for EGFR/Ras activity in proliferation (Tseng et al., 2007). In mammals, it has been demonstrated that CIC forms a stable protein complex with ATXN-1, which is involved in neurodegenerative diseases (Lam et al., 2006). Moreover, CIC is found to form a chimeric protein with Double Homeobox protein 4 (DUX4) in a subset of Ewing-like sarcomas, implicating CIC in cancer (Kawamura-Saito et al., 2006). Despite the clear genetic evidence, molecular mechanisms by which CIC contributes to human disorders remain elusive.

Here, we report that Cic cooperates with RBF1 to restrict proliferation during *Drosophila* eye development. We demonstrate that Cic, together with RBF1, represses Cyclin E expression and promotes G1 arrest in asynchronously dividing precursor cells as they enter the MF. Moreover, we show that *cic* mutations can promote the survival of *rbf1* mutant cells, which was previously shown to be EGFR/Ras dependent. Strikingly, further investigation of the pro-survival effect of *cic* mutations revealed that Cic regulates the level of reactive oxygen species (ROS), which are able to modulate the sensitivity of *rbf1* mutant cells to undergo cell death. Our results provide evidence to demonstrate the importance of the crosstalk between the EGFR/Ras and RBF1 pathways in coordinating cell cycle progression and survival during *Drosophila* eye development.

Results

In third instar *Drosophila* eye imaginal discs, S-phase cells can be observed in two mitotic waves (Baker, 2001). The first mitotic wave is composed of asynchronously dividing cells towards the anterior of the disc. These cells are subsequently arrested in G1 at the morphogenetic furrow (MF) and a fraction of them begin to differentiate. Cells that are not differentiating at the MF enter one more round of synchronous S-phase towards the posterior of the MF, representing the second mitotic wave (SMW). In setting out to further comprehend how RBF1 controls the cell cycle in the eye imaginal disc, we generated mitotic clones of an *rbf1* null allele, $rbf1^{\Delta 14}$, in an eye-specific manner. Subsequently, third instar larval eye imaginal discs were dissected and fluorescently labelled with EdU, which allows visualisation of S-phase cells. We frequently observed *rbf1* null clones with and without ectopic S-phase cells at the MF in a single eye imaginal disc (Fig. 1, asterisk and arrowhead). This result suggests that factors other than RBF1 are at play to promote G1 arrest at the MF. Notably, Dacapo (Dap), a Cyclin Dependent Kinase inhibitor, has been previously shown to cooperate with RBF1 to maintain photoreceptors in G1 phase of the cell cycle (Firth and Baker, 2005). However, immunostaining with anti-Dap revealed that Dap proteins are expressed at a relatively low level in the anterior region of the MF, raising the possibility that factors other than Dap might maintain *rbf1* mutant cells in G1 in the anterior region of the MF (Fig. 1).

We began to explore factors downstream of the EGFR/Ras pathway that might synergize with RBF1 to promote cell cycle arrest. A candidate upon which we narrowed our focus was an HMG box transcription factor called Capicua (Cic). Similar to Dap, Cic is a negative regulator of proliferation whose expression is controlled by the EGFR/Ras pathway (Astigarraga et al., 2007). We first examined the expression pattern of Cic in eye imaginal discs by co-immunostaining for Cic and a nuclear protein Eyes Absent (Eya), which we used to visualise the nucleus of cells at the MF. As shown in Fig. 2A, Cic is expressed

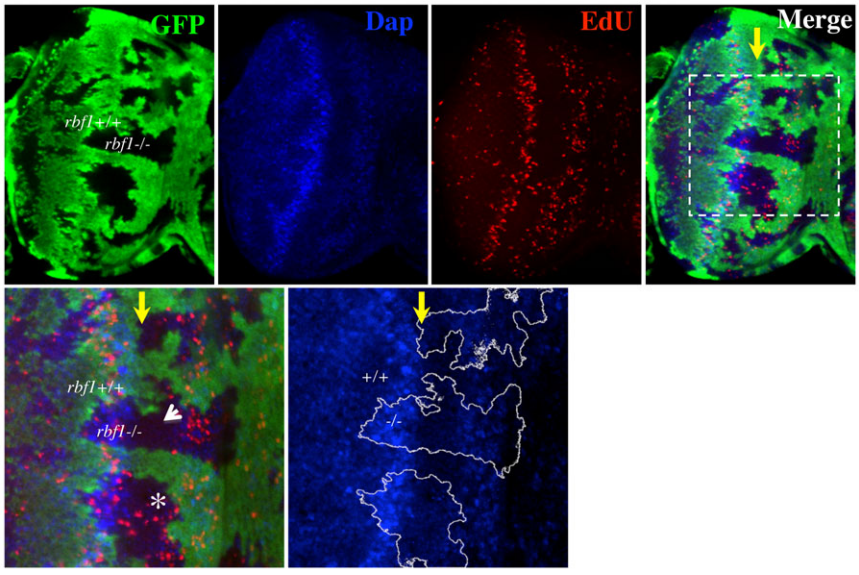

Fig. 1. *rbf1* mutant cells arrest in G1 at the morphogenetic furrow (MF). Mosaic clones of an *rbf1* null allele, $rbf1^{\Delta 14}$, were generated in third instar eye imaginal discs using *eyFLP*. $rbf1^{\Delta 14}$ mutant clones are marked by the lack of GFP signal (green). Fluorescently labelled EdU (see Materials and Methods) was used to mark S-phase cells (red) and anti-Dacapo was used to determine the expression pattern of Dacapo (blue) in the eye disc. The position of the MF is indicated by a yellow arrow. A magnified view of the indicated area (white box) is presented below. Note that some *rbf1* mutant clones contained S-phase cells at the MF (asterisk) while others do not (arrowhead).

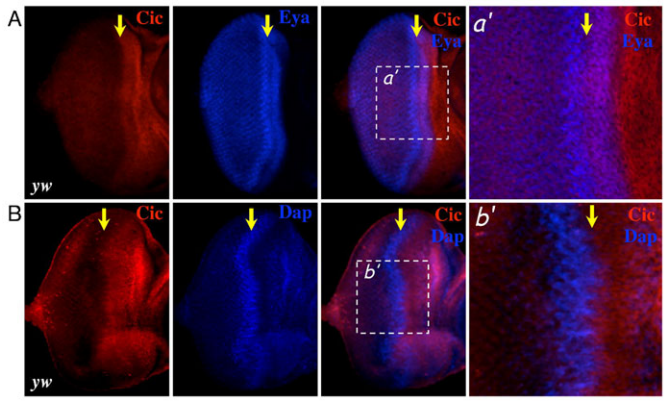

Fig. 2. Expression pattern of Capicua in the third instar eye imaginal disc. Third instar eye imaginal discs from *yw* flies are co-immunostained (**A**) with anti-Capicua (red) and anti-Eye Absence (blue) or (**B**) with anti-Capicua (red) and anti-Dacapo (blue). The position of the MF is indicated by a yellow arrow. Right panels show magnified views of the indicated areas (white box).

in the progenitor cells anterior to the MF as well as in the cells within the anterior half of the MF. Cic expression sharply decreases in the posterior half of the MF. Interestingly, eye discs co-immunostained for Cic and Dap reveal that Cic expression clearly declines where Dap proteins are highly expressed (Fig. 2B). These expression patterns suggest that the cellular context in which Cic functions as a negative regulator of proliferation might be distinct from that of Dap, and that Cic might be important for controlling proliferation in progenitor cells, including the cells at the anterior region of the MF.

To explore whether Cic cooperates with RBF1 to promote G1 arrest, we examined the consequences of inactivating Cic in an *rbf1* mutant background. As homozygous *rbf1* null flies die at the first instar larval stage, we took advantage of an *rbf1* hypomorphic allele, $rbf1^{120a}$. Eye discs containing mutant clones of *cic* were generated in either a control or $rbf1^{120a}$ background. These eye discs were fluorescently labelled with EdU and subsequently immunostained for Atonal (Ato) to visualise S-phase cells and differentiating cells respectively. As previously reported, *cic* mutation alone cannot overcome the developmentally regulated G1 arrest at the MF (Fig. 3A) (Tseng et al., 2007). In contrast, *rbf1 cic* double mutant cells are capable of entering S phase in the MF. We also observed that the pattern of S-phase cells in the SMW is disrupted in the double mutant clones, which could be a secondary consequence of failure to arrest at the MF. Of note, we did not observe EdU staining in cells with high levels of Ato, indicating that once the differentiation process has begun, *rbf1 cic* double mutant cells remain arrested in G1. To better visualise the cell cycle defect, we generated eye discs entirely composed of *cic* single or *rbf1 cic* double mutant cells (see Materials and Methods). As expected, we did not observe any ectopic S-phase cells in *cic* mutant eye discs while ectopic S-phase cells are discernible in *rbf1 cic* double mutant eye discs (supplementary material Fig. S1B). We used these *rbf1 cic* double mutant eye discs to quantify the number of ectopic S-phase cells in the MF and compared it to *rbf1* mutant eye discs where we also occasionally observed ectopic S-phase cells (supplementary material Fig. S1C). Because the size of the MF varies between eye discs, we normalised the number of EdU positive cells by the size of the MF. This was

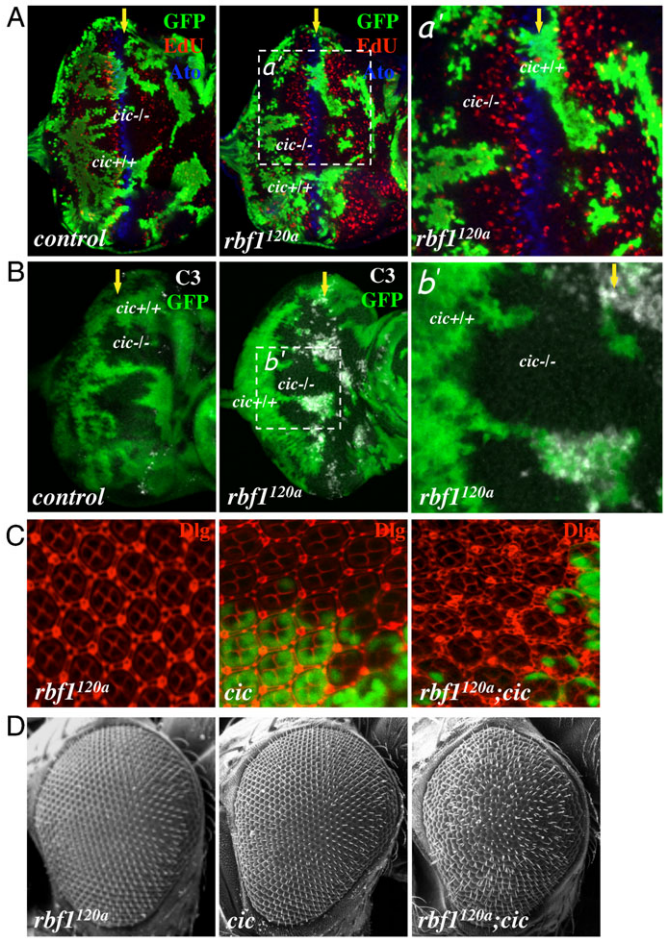

Fig. 3. *cic* mutations cooperate with *rbf1* mutation to promote proliferation and survival. (**A**) Mosaic clones of *cic* mutant cells were generated in control or $rbf1^{120a}$ mutant eye discs. Third instar eye imaginal discs were then incubated with EdU (red) to visualise S-phase cells and immunostained with anti-Atonal (blue). *cic* mutant clones are marked by the lack of GFP signal (green) and the position of the MF is marked by a yellow arrow. (**B**) Eye imaginal discs of the same genotypes as in A are shown. Anti-cleaved Caspase 3 (C3) was used to detect apoptotic cells (white). (**C**) Pupal eye discs (42 hours after pupal formation (APF)) of $rbf1^{120a}$ mutant flies, flies with *cic* mutant clones and $rbf1^{120a}$ mutant flies that contain *cic* mutant clones were immunostained with anti-Discs Large (red). (**D**) Scanning Electron Microscopy (SEM) images of *Drosophila* adult eyes entirely composed of $rbf1^{120a}$ or *cic* single mutant cells and $rbf1^{120a}$ *cic* mutant cells are presented.

achieved by measuring the number of pixels in images taken at the same magnification. We determined that on average 1.6 ± 0.67 ectopic S-phase cells/10,000 pixels are present in *rbf1* single mutant discs while 4.55 ± 0.75 ectopic S-phase cells/10,000 pixels are present in *rbf1 cic* double mutant eye discs, showing a 2.8 fold increase. This result demonstrates that Cic and RBF1 collectively promote G1 arrest at the MF.

We also investigated the possibility that Cic regulates survival of *rbf1* mutant cells. Normally, *rbf1* mutant cells undergo cell death in the anterior region of the MF (Moon et al., 2005; Tanaka-Matakatsu et al., 2009). Intriguingly, immunostaining with anti-cleaved Caspase-3 (C3), which marks apoptotic cells, revealed that the *rbf1 cic* double mutant cells no longer undergo cell death at the MF (Fig. 3B). In order to better visualise these pro-proliferative and pro-survival effects of the *cic* mutation on *rbf1* mutant cells, we decided to examine the pupal eye. A typical

ommatidial cluster at 42 hours after pupal formation (APF) contains 8 photoreceptors that are surrounded by accessory cells: 4 cone cells, 2 primary pigment cells, 6 secondary pigment cells and 3 tertiary pigment cells (Baker, 2001). Anti-Discs Large was used to visualise the cellular outlines in control and $rbf1^{120a}$ pupal eye discs. As shown in Fig. 3C, *rbf1 cic* double mutant ommatidial clusters display a great surplus of interommatidial cells, while only a few *cic* single mutant ommatidial clusters contain extra interommatidial cells. As a result, *rbf1 cic* double mutant adult eyes display a strong rough eye phenotype, which is not apparent in either *rbf1* or *cic* single mutant adult eyes (Fig. 3D). Overall, our results suggest that *cic* mutations promote ectopic proliferation and survival in $rbf1^{120a}$ mutant eyes.

In an effort to understand how *cic* mutations might cooperate with *rbf1* mutations to overcome G1 arrest, we considered the role of Cyclin E, which is a well-known target of RBF1. In developing eye imaginal discs, the expression pattern of Cyclin E largely reflects the global distribution of S-phase cells, exhibiting reduced expression in the MF and high levels of expression at the SMW (Fig. 4A). Surprisingly, we observed that reducing the gene dosage of *rbf1* by half was sufficient to derepress Cyclin E expression at the MF (Fig. 4B). In $rbf1^{120a}$ heterozygous eye discs, cells with high levels of Cyclin E expression are more frequently observed compared to control eye discs. However, the cells at the SMW still display the highest level of Cyclin E expression in the $rbf1^{120a}$ heterozygous eye discs. With this is mind, we sought to use $rbf1^{120a}$ heterozygous eye discs as a sensitised genetic background to determine if RBF1 and Cic cooperate to control Cyclin E levels. In order to test this, we generated $rbf1^{120a}$ heterozygous eye discs carrying *cic* homozygous mutations using the methods described previously (see Materials and Methods). As shown in Fig. 4C, *cic* mutant cells with *rbf1* heterozygous mutations exhibit augmented levels of Cyclin E expression at the MF comparable to the level observed at the SMW. It almost appears as if the SMW is anteriorly expanded. This effect of *cic* mutations on Cyclin E expression was not evident in the wild-type background, indicating that RBF1 function must be compromised for *cic* mutations to have an effect on Cyclin E expression (data not shown). Importantly, the increase in Cyclin E expression in the $rbf1^{120a}$ heterozygous background is not simply a consequence of ectopic S-phase cells since *cic* mutant cells in the $rbf1^{120a}$ heterozygous background properly arrest in G1 at the MF (supplementary material Fig. S1). Since *cyclin E* is a well-known transcriptional target of RBF1 and the effect of *cic* mutations on Cyclin E levels could be observed in the $rbf1^{120a}$ heterozygous background, we predicted that Cic would impinge on *cyclin E* transcription. Therefore, we performed RT-qPCR using eye discs from the genotypes in which we detected a difference in the Cyclin E protein level (supplementary material Fig. S2C). However, we did not observe any appreciable changes in the RNA level, indicating that the effect of *cic* mutations on Cyclin E expression is likely post-transcriptional. Nevertheless, our result suggests that RBF1 and Cic cooperatively promote G1 arrest at the MF, at least in part, by limiting Cyclin E expression.

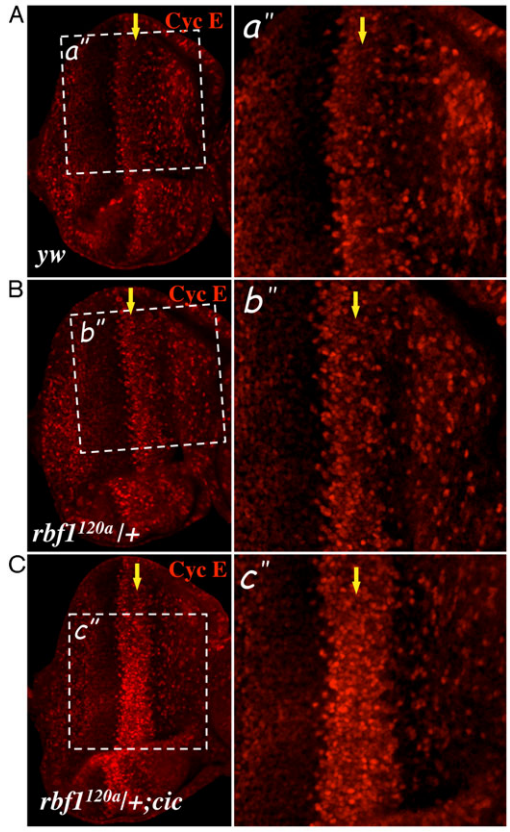

Fig. 4. Cyclin E expression is deregulated in *cic* mutant clones. Control (*yw*) and $rbf1^{120a}$ heterozygous (+/$rbf1^{120a}$) eye discs and $rbf1^{120a}$ heterozygous eye discs also carrying *cic* homozygous mutations were immunostained with anti-Cyclin E (magenta). The position of the MF is marked by a yellow arrow. Magnified views of the indicated areas (white box) are also presented.

During the course of our study, an article was published demonstrating that Bantam miRNA expression is elevated in *cic* mutant cells (Herranz et al., 2012). Bantam miRNA has been shown to inhibit Hid expression (Brennecke et al., 2003), lending an explanation as to why *cic* mutations can inhibit the ectopic cell death in *rbf1* mutant eye discs. However, this does not exclude the possibility that Cic possesses other cellular functions that could contribute to its pro-survival effect on *rbf1* mutant cells. A handful of recent studies in mammals have made connections between RB and metabolic stress. E2F-1 and RB have proven to be a requirement for the repression of genes involved in oxidative metabolism, and inactivation of the tumour suppressor gene TSC2 induces cell death in RB-deficient cancer cells by promoting oxidative stress (Blanchet et al., 2011; Li et al., 2010). Hence, we set out to test whether *cic* and/or *rbf1* loss had any discernible effect on reactive oxygen species (ROS) production. Eye discs containing homozygous mutant clones of either *rbf1* or *cic* were generated and stained with dihydroethidium (Dhe) to monitor the levels of ROS. $rbf1^{\Delta 14}$ clones showed no consistent difference in ROS levels (Fig. 5A). Contrastingly, mutant clones for *cic* showed a decrease in ROS levels in both wild-type and $rbf1^{120a}$ homozygous mutant backgrounds, suggesting that Cic is required for proper ROS homeostasis (Fig. 5).

The decrease in ROS levels could simply be a consequence of *cic* mutations and may not contribute to the cell cycle and cell death phenotypes observed in *rbf1 cic* double mutant clones. Alternatively, these decreased ROS levels could directly contribute to the phenotypes. In order to distinguish between these two possibilities, we altered the ROS level in *rbf1* mutant eye discs by modulating levels of ROS scavenger enzymes. To increase ROS levels, we expressed a Superoxide Dismutase 2

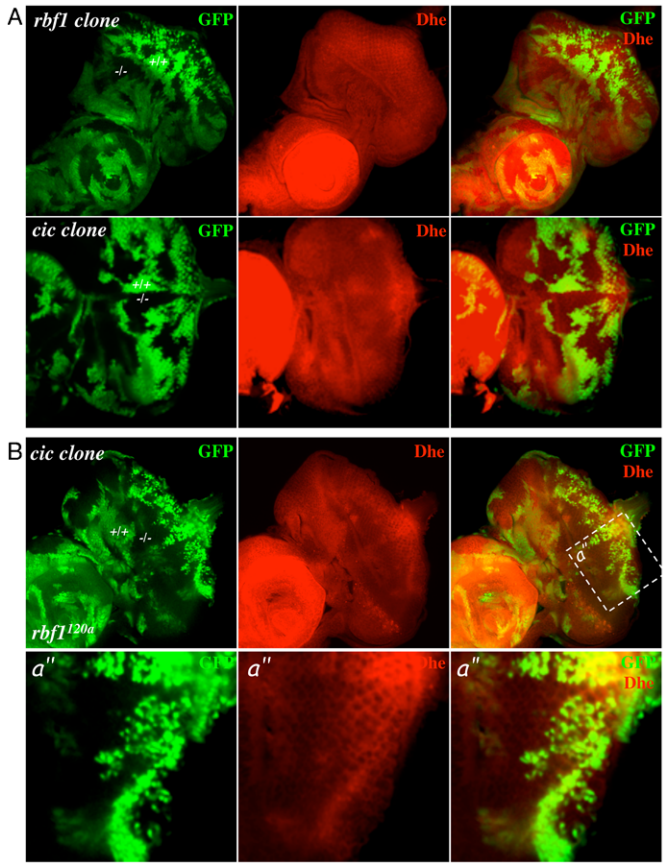

Fig. 5. Cic mutant cells have a low level of Reactive Oxygen Species (ROS). (**A**) Third instar eye discs containing mosaic clones of either *rbf1* null mutant cells or *cic* mutant cells were stained with Dihydroethidium (Dhe) to monitor the levels of ROS. Note that the intensity of Dhe staining is weaker in *cic* mutant clones compared to the wild-type clones while it is relatively similar between the *rbf1* mutant and control clones. (**B**) Mosaic clones of *cic* mutant cells were generated in $rbf1^{120a}$ mutant flies. Third instar eye imaginal discs were stained with Dhe to monitor the level of ROS. Magnified views of the indicated areas (white box) are also presented.

(SOD2) RNAi construct in $rbf1^{120a}$ eye discs. We observed that the stripe of cell death at the MF of $rbf1^{120a}$ eye discs, visualised by anti-C3, becomes wider when SOD2-RNAi is expressed (Fig. 6A). Importantly, there is no apparent increase in cell death when SOD2-RNAi was expressed in a wild-type background, indicating that the effect of SOD2-RNAi is *rbf1* specific. Next, in order to test the outcome of reducing ROS, we overexpressed SOD2 in $rbf1^{120a}$ eye discs. We observed inconsistent results with larval eye discs where some eye discs show weak or partial decrease in cell death, while others show no change. Therefore, we decided to study pupal eye discs since the stereotypical organisation of an ommatidial cluster facilitates visualisation of defects in cell number. Pupal eye discs 42 hours APF were immunostained with anti-Discs Large (Fig. 6B). We observed that SOD2 overexpression in *rbf1* mutant eyes can result in ommatidial clusters with extra interommatidial cells (Fig. 6B). However, because this effect seems to vary among the discs, and because we did observe that SOD2 overexpression can have an effect in the wild type eye discs, we quantified the ommatidial defect. For each genotype, we counted ommatidia with six secondary pigment cells, which is expected from wild type, and ommatidia with either less or more than six secondary pigment cells. This was done for random regions of ~10 pupal eye discs for each genotype. As shown in Fig. 6C, SOD2 overexpression produces more ommatidia with extra interommatidial cells in the *rbf1* mutant background than in the wild type background (24% in wild type and 46% in *rbf1* mutant). Because 22% of the *rbf1* mutant ommatidia already have extra interommatidial cells, the effect of SOD2 overexpression in the *rbf1* mutant background could be additive. Nevertheless, our results collectively suggest that changes in ROS levels can influence the cell death phenotype in *rbf1* mutant eyes and likely contribute to the pro-survival effect of *cic* mutations.

Discussion

We report here that a downstream effector of the EGFR/Ras pathway, Cic, is an important determinant of proliferation and survival of RB-deficient cells in *Drosophila*. We provide evidence to suggest that Cic synergizes with RBF1 to restrict Cyclin E expression at the MF and that Cic controls ROS levels that can influence the cell death phenotype in *rbf1* mutant eyes. Our study strengthens the idea that extensive crosstalk exists between EGFR/Ras and RBF1, and demonstrates the importance of coordinating their functions during development.

Both Dap and Cic are negative regulators of proliferation downstream of the EGFR/Ras pathway. However, EGFR/Ras activity promotes Dap expression while inhibiting Cic expression (Astigarraga et al., 2007; Firth and Baker, 2005). Accordingly, their expression patterns at the MF show that Cic expression drops where Dap expression is most prominent. Immunostaining with anti-phospho-MAPK, which is a marker for EGFR activity and cells initiating differentiation processes, shows a similar expression pattern to that of Dap (Gabay et al., 1997). Perhaps, once cells start to differentiate, Dap plays a predominant role over Cic to maintain differentiating cells in the G1 phase. This would also explain the absence of EdU-positive cells in *rbf1 cic* double mutant clones that express Atonal (Fig. 3A). We noticed that Dap expression is slightly increased in *rbf1* mutant clones. This is likely in response to the Cyclin E activation, a phenomenon which has been previously reported (de Nooij et al., 2000). In contrast to the MF, we could detect co-expression of Dap and Cic proteins in the anterior region of the eye disc (Fig. 2). Perhaps, in this region, EGFR/Ras is activated to a level at which both proteins can coexist. Nevertheless, our results indicate that, at least at the MF, the cellular context in which Dap and Cic act to restrict proliferation is distinct.

In *cic* homozygous mutant eye discs generated in the $rbf1^{120a}$ heterozygous background, Cyclin E levels are specifically increased at the MF (Fig. 4C). In fact, this is the location where dE2F1 proteins are most highly expressed in the eye disc (Moon et al., 2006). While this observation suggests a strong cooperation between dE2F1 and Cic, we did not observe any change in the dE2F1 protein level nor its activity in *cic* mutant clones (supplementary material Fig. S2). This result indicates that *cic* mutations do not affect dE2F1 activity in general. A previous study demonstrated that increases in both Cyclin E and E2F activities are necessary to overcome the cell cycle arrest imposed at the MF (Firth and Baker, 2005). This likely explains why we did not observe ectopic S-phase cells in *cic* mutant cells generated in $rbf1^{120a}$ heterozygous eye discs despite the elevated level of Cyclin E expression (supplementary material Fig. S1). E2F target genes are consistently expressed at a lower level in *cic* mutant eye discs

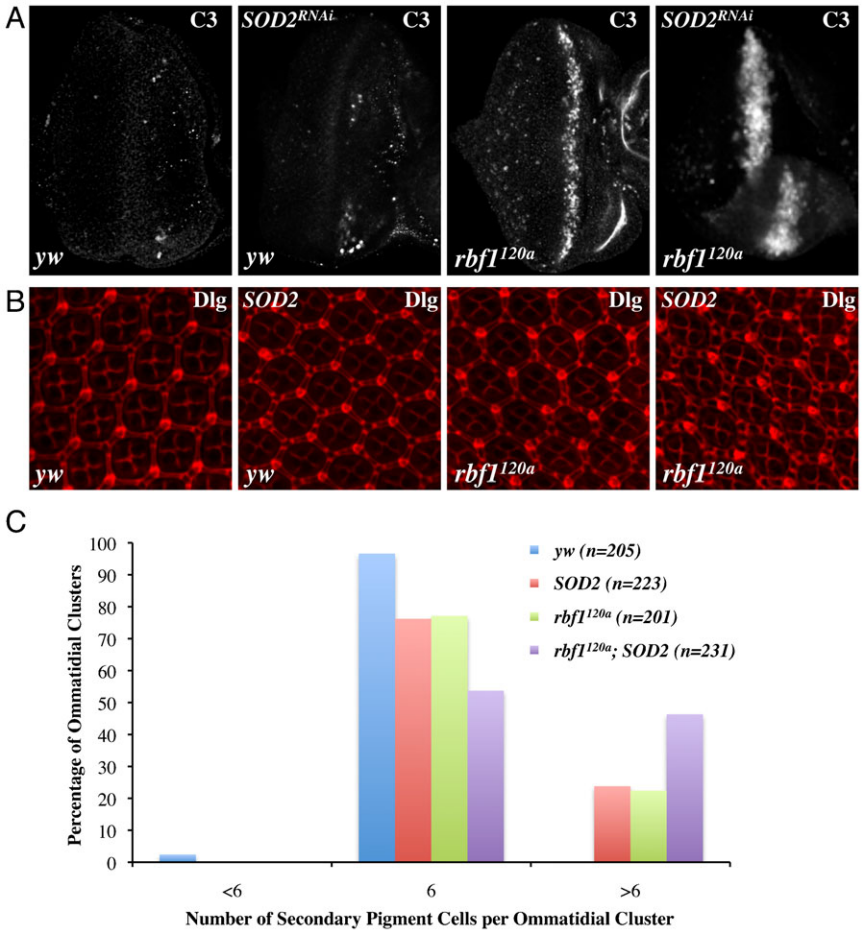

Fig. 6. SOD2 can promote the survival of *rbf1* mutant cells. (**A**) Third instar eye discs expressing dsRNA against Superoxide Dismutase 2 (SOD2) in either *yw* or $rbf1^{120a}$ backgrounds were immunostained with anti-C3. (**B**) Eye discs (42 hours APF) from flies overexpressing SOD2 in either *yw* or $rbf1^{120a}$ backgrounds were immunostained with anti-Discs Large. (**C**) The percentage of ommatidia with abnormal secondary pigment cells was determined for *yw*, *SOD2*, $rbf1^{120a}$ and $rbf1^{120a}$; *SOD2* pupal eye discs. In a control background 97% of ommatidial clusters have 6 secondary pigment cells, which is normally expected. However, in an $rbf1^{120a}$ background overexpressing SOD2, 46.3% of ommatidial clusters have greater than 6 secondary pigment cells. *SOD2* and $rbf1^{120a}$ pupal eye discs contain 24% and 22% of ommatidial clusters with extra interommatidial cells respectively.

generated in the $rbf1^{120a}$ heterozygous background than $rbf1^{120a}$ homozygous mutant eye discs (supplementary material Fig. S2). Nevertheless, we cannot exclude the possibility that dE2F1 is required for the effect of *cic* mutations on Cyclin E expression. It is interesting to note that both Dap and Cic act on Cyclin E/CDK2 and that their mutations cooperate with *rbf1* mutations to cause uncontrolled proliferation. Perhaps, such a context in which either E2F1 or Cyclin E/CDK2 activity is elevated represents a sensitised genetic background where regulators of the other protein can be identified. Indeed, haploinsufficiency of *rbf1* is shown to be sufficient to dominantly modify the rough eye phenotype induced by p21 overexpression, the mammalian inhibitor of Cyclin E/CDK2 (Du and Dyson, 1999).

The molecular mechanism by which RBF1 and Cic cooperatively regulate Cyclin E expression remains unclear. RT-qPCR did not reveal that *cic* mutations produce any discernable changes in *cyclin E* RNA levels, indicating that the effect of *cic* mutations on Cyclin E expression is post-transcriptional and likely to be indirect. One interesting observation is that heterozygosity of *rbf1* seems to have a general effect on the expression level of RBF1 target genes (supplementary material Fig. S2B). Transcript levels of *mcm2* and *rnrS* are elevated in the *rbf1* heterozygous background compared to the wild type. This raises the possibility that increased expression of RBF1 target genes in general provides a specific context that allows the *cic* mutation to have an effect on Cyclin E expression. We are currently investigating the transcriptional changes that are induced by *cic* mutations in control and *rbf1* mutant backgrounds to determine if Cic regulates different transcriptional programs depending on the status of RBF1.

Whether the alteration of Cyclin E levels is the only molecular mechanism by which *cic* and *rbf1* mutations cooperate to promote ectopic S phase is still unclear. Oddly, we could not detect any discernible change in Cyclin E levels when *cic* mutant clones were generated in an $rbf1^{120a}$ homozygous background despite the presence of ectopic S-phase cells. One possible explanation for this is that *rbf1* homozygous mutations increase Cyclin E expression to the level higher than what is achieved by *cic* mutations in $rbf1^{120a}$ heterozygous backgrounds. This increase is perhaps near, but not over, the threshold that can overcome the G1 arrest at the MF. In this context, *cic* mutations would provide the additional Cyclin E expression that is required to actually surpass this threshold. However, once cells enter S phase, Cyclin E is rapidly targeted for degradation, making it difficult to detect the increase in Cyclin E level. The lack of an increase in Cyclin E level in the $rbf1^{120a}$ homozygous background could also indicate that *cic* mutations can result in additional molecular changes that can cooperate with *rbf1* mutations. While it is unclear what these changes might be, we know that Cic's ability to regulate ROS is not likely to contribute to the cell cycle defect. We did not observe any changes in the EdU staining pattern when expression levels of SOD2 were altered in an *rbf1* mutant background (data not shown). Presently,

we are in the process of comparing transcriptional changes induced by *cic* mutations in wild-type and *rbf1* mutant backgrounds in order to postulate a molecular mechanism.

One of the unforeseen findings from our study is that ROS homeostasis is regulated by Cic. Reduced levels of ROS in *cic* mutant cells was not simply a secondary consequence of overcoming G1 arrest since *cic* mutant clones display normal patterns of proliferation in wild-type eye discs (Fig. 3A). Moreover, the changes in ROS levels are most evident at the posterior region of the MF where most cells are arrested in the G1 phase (Fig. 5). We measured the transcript levels of *sod1*, *sod2*, and *catalase* in a *cic* mutant background to determine if Cic controls ROS levels by regulating transcription of ROS scavenger enzymes. However, we did not observe any changes in their RNA levels, suggesting that Cic regulates ROS levels through an alternative mechanism (supplementary material Fig. S3). While this mechanism is still unclear, it is interesting to note that CIC in mammals is a component of the protein complex that includes Ataxin-1 (Atxn1), which is involved in Spinocerebellar Ataxia (Lam et al., 2006). A recent study demonstrated that *CIC* mutations can provide improvement of disease phenotypes observed in a polyglutamine-expanded Atxn1 mouse model (Fryer et al., 2011). It will be interesting to investigate if CIC regulates ROS levels in this biological context as well, and whether changes in ROS levels contribute to the effect of *CIC* mutations on the neurodegenerative phenotype.

Another interesting aspect of CIC in mammals is that CIC likely plays an important role in human cancers. In addition to the CIC–DUX4 chimeric protein mentioned in the introduction, a recent study revealed that *CIC* is somatically mutated in six out of seven oligodendroglioma patients (Bettegowda et al., 2011). Despite its possible involvement in human cancer, *CIC* knockout mice were reported to have no obvious tumour phenotype (Lee et al., 2011). It will be particularly interesting to test if *CIC* mutations can modify the tumour phenotypes of RB-deficient mice. Evidently, CIC is involved in a variety of important biological processes and warrants further investigation.

Materials and Methods

Fly stocks

All fly crosses were performed at 25℃. The *rbf1* mutants, $rbf1^{120a}$ and $rbf1^{\Delta 14}$ have been previously described (Du and Dyson, 1999). The *cic* allele used in this study is cic^{Q474X} (Tseng et al., 2007). The *SOD2* RNAi allele and the *UAS-SOD2* allele were obtained from the Bloomington Stock Center.

Mosaic clones

$rbf1^{\Delta 14}$*FRT19A/*GFP^{Ubi}*FRT19A*; *eyFLP/+*
$rbf1^{120a}$*eyFLP/Y*; *FRT82B* GFP^{Ubi}*/FRT82B* cic^{Q474X}
yw eyFLP/Y; *FRT82B* GFP^{Ubi}*/FRT82B* cic^{Q474X}
$rbf1^{120a}$ *eyFLP/+*; *FRT82B* GFP^{Ubi}*/FRT82B* cic^{Q474X}

SOD2 flies

$rbf1^{120a}$ *eyFLP/Y*; *Act <CD2 <GAL4, UAS-GFP/SOD2 RNAi*
yw eyFLP/Y; *Act <CD2 <GAL4, UAS-GFP/SOD2 RNAi*
$rbf1^{120a}$*eyFLP/Y*; *Act <CD2 <GAL4, UAS-GFP/UAS-SOD2*
yw eyFLP/Y; *Act <CD2 <GAL4,UAS-GFP/UAS-SOD2*

Generation of eye discs entirely composed of cic mutant cells

ey-FLP/+ ; FRT 82B P(W+) l(3)cl-R3/FRT82B cic^{Q474X}
$rbf1^{120a}$ *ey-FLP/+*; *FRT 82B P(W+) l(3)cl-R3/FRT82B* cic^{Q474X}
$rbf1^{120a}$ *ey-FLP/Y ; FRT 82B P(W+) l(3)cl-R3/FRT82B* cic^{Q474X}

Immunostaining

The following antibodies were used in this study: anti-C3 (1/200, Cell Signaling), anti-Dacapo (1/100, Developmental Studies Hybridoma Bank, DSHB), anti-Eyes Absent (1/100, DSHB) anti-Discs Large (1/100, DSHB), anti-Capicua (1/1000, a gift from Dr I. Hariharan), anti-Atonal (1/300, a gift from Dr Y.N. Jan), anti-Cyclin-E (1/100. a gift from Dr H. McNeill and Santa Cruz Bio.), anti-dE2F1 (1/1000, a gift from Dr N.J. Dyson).

For immunostaining, third larval instar or pupal eye discs were dissected and fixed with 4% paraformaldehyde for 20 to 30 minutes at room temperature. Next, discs were washed twice with 0.3% PBST (0.3% Triton X-100 in PBS) for 10 minutes. Eye discs were then incubated with primary antibody in 0.1% PBST with 5% normal goat serum (NGS) at room temperature for 2 hours. Eye discs were washed five times with 0.1% PBST and incubated with secondary antibody in 0.3% PBST with 5% NGS for 2 hours at room temperature. The immunostained discs were then washed five times with 0.1% PBST at room temperature and mounted for confocal microscopy imaging (Zeiss LSM).

EdU labeling

To visualise S-phase cells, Ethynyl-2′-Deoxyuridine (EdU) cell proliferation assay from Invitrogen was used with the following modification. Eye discs were dissected at the third larval instar stage and incubated in Schneider's medium containing EdU for 1 hour at room temperature. Eye discs were washed two times with 1× PBS and fixed at room temperature in 4% paraformaldehyde for 20 minutes. After fixation, eye discs were washed with PBS containing 3% BSA two times for 5 minutes. Eye discs were then incubated with the detection cocktail according to the manufacturer's specifications. Eye discs were treated with appropriate antibodies for immunostaining and mounted for confocal microscopy.

Real-time quantitative RT-PCR

Total RNA was isolated from 40 eye-antenna discs with RNeasy Mini Kit (QIAGEN) according to the manufacturer's specifications. RNA was reverse transcribed using DyNAmo cDNA Synthesis Kit (Finnzymes). DyNAmo Flash SYBR Green qPCR kit was subsequently used to perform quantitative PCR reactions. *RP49* and *β-tubulin* were used as normalisation controls. Primers were designed with Primer3 (Whitehead Institute for Biomedical Research primer3 shareware [http://primer3.wi.mit.edu]). Primer pairs used were:

SOD1-Forward (ATTAACGGCGATGCCAAG) and SOD1-Reverse (ATTGGTGTTGTCACCGAACTC), SOD2-Forward (CGTAAAATTTCGCAAACTGC) and SOD2-Reverse (GTAGGTCTGGTGGTGCTTCTG), Catalase-Forward (ATCCCGTTGAGCAAATATCC) and Catalase-Reverse (AGGCATCCTTGATTCCAATG), Cyclin E-Forward (GTTTGTGCAAACCTCACAGT) and Cyclin E-Reverse (AACAGCGTAAAGCCATCTCC), Mcm2-Forward (AGGAACCACAGCTGAAGACC) and Mcm2-Reverse (CGTACATCTTGGCGATCTTG), RnrS Forward (AATGGCGTCCAAGGAAAAC) and RnrS Reverse (ACATCTTGCGAACGTTGTTG), β-tubulin-Forward (ACATCCCGCCCCGTGGTC) and β-tubulin-Reverse (AGAAAGCCTTGCGCCTGAACATAG), Rp49-F (TACAGGCCCAAGATCGTGAAG) and Rp49-R (GACGCACTCTGTTGTCGATACC).

Dhe staining

Dihydroethidium (Dhe) dye was reconstituted in 1 ml Schneider's medium to give a final concentration of 30 µM. Eye discs were subsequently incubated in solution for 5 minutes at room temperature in a dark chamber. Then three 5-minute washes were performed in 1 ml Schneider's medium. Discs were fixed for 5 minutes in 4% paraformaldehyde and washed once with 1× PBS for 5 minutes. Confocal microscopy was used to visualise the Dhe staining.

Acknowledgements

We would like to thank Dr Iswar Hariharan for providing us with *cic* stocks and antibodies. We would also like to thank Dr Helen McNeill and Dr Yuh Nung Jan for sharing their antibodies. Thanks to Bloomington Stock Center for providing the fly stocks and Developmental Studies Hybridoma Banks at the University of Iowa for antibodies. This study was supported by Canada Institute for Health Research grant MOP-93666, Natural Science and Engineering Research Council of Canada grant 355760-2008. N.-S.M. is a recipient of CIHR New Investigators Salary Award and M.-R.B.-G. is a recipient of NSERC Alexander Graham Bell Scholarship.

Competing Interests

The authors have no competing interests to declare.

References

Astigarraga, S., Grossman, R., Díaz-Delfín, J., Caelles, C., Paroush, Z. and Jiménez, G. (2007). A MAPK docking site is critical for downregulation of Capicua by Torso and EGFR RTK signaling. *EMBO J.* **26**, 668-677.

Baker, N. E. (2001). Cell proliferation, survival, and death in the *Drosophila* eye. *Semin. Cell Dev. Biol.* **12**, 499-507.

Bergmann, A., Agapite, J., McCall, K. and Steller, H. (1998). The *Drosophila* gene *hid* is a direct molecular target of Ras-dependent survival signaling. *Cell* **95**, 331-341.
Bettegowda, C., Agrawal, N., Jiao, Y., Sausen, M., Wood, L. D., Hruban, R. H., Rodriguez, F. J., Cahill, D. P., McLendon, R., Riggins, G. et al. (2011). Mutations in *CIC* and *FUBP1* contribute to human oligodendroglioma. *Science* **333**, 1453-1455.
Blanchet, E., Annicotte, J. S., Lagarrigue, S., Aguilar, V., Clapé, C., Chavey, C., Fritz, V., Casas, F., Apparailly, F., Auwerx, J. et al. (2011). E2F transcription factor-1 regulates oxidative metabolism. *Nat. Cell Biol.* **13**, 1146-1152.
Bowles, E., Corson, T. W., Bayani, J., Squire, J. A., Wong, N., Lai, P. B. and Gallie, B. L. (2007). Profiling genomic copy number changes in retinoblastoma beyond loss of *RB1*. *Genes Chromosomes Cancer* **46**, 118-129.
Brennecke, J., Hipfner, D. R., Stark, A., Russell, R. B. and Cohen, S. M. (2003). *bantam* encodes a developmentally regulated microRNA that controls cell proliferation and regulates the proapoptotic gene *hid* in *Drosophila*. *Cell* **113**, 25-36.
de Nooij, J. C., Graber, K. H. and Hariharan, I. K. (2000). Expression of the cyclin-dependent kinase inhibitor Dacapo is regulated by cyclin E. *Mech. Dev.* **97**, 73-83.
Dimova, D. K. and Dyson, N. J. (2005). The E2F transcriptional network: old acquaintances with new faces. *Oncogene* **24**, 2810-2826.
Du, W. and Dyson, N. (1999). The role of RBF in the introduction of G_1 regulation during *Drosophila* embryogenesis. *EMBO J.* **18**, 916-925.
Dyson, N. (1998). The regulation of E2F by pRB-family proteins. *Genes Dev.* **12**, 2245-2262.
Firth, L. C. and Baker, N. E. (2005). Extracellular signals responsible for spatially regulated proliferation in the differentiating *Drosophila* eye. *Dev. Cell* **8**, 541-551.
Fryer, J. D., Yu, P., Kang, H., Mandel-Brehm, C., Carter, A. N., Crespo-Barreto, J., Gao, Y., Flora, A., Shaw, C., Orr, H. T. et al. (2011). Exercise and genetic rescue of SCA1 via the transcriptional repressor Capicua. *Science* **334**, 690-693.
Gabay, L., Seger, R. and Shilo, B. Z. (1997). In situ activation pattern of *Drosophila* EGF receptor pathway during development. *Science* **277**, 1103-1106.
Herranz, H., Hong, X. and Cohen, S. M. (2012). Mutual repression by bantam miRNA and Capicua links the EGFR/MAPK and Hippo pathways in growth control. *Curr. Biol.* **22**, 651-657.
Jiménez, G., Shvartsman, S. Y. and Paroush, Z. (2012). The Capicua repressor – a general sensor of RTK signaling in development and disease. *J. Cell Sci.* **125**, 1383-1391.
Kawamura-Saito, M., Yamazaki, Y., Kaneko, K., Kawaguchi, N., Kanda, H., Mukai, H., Gotoh, T., Motoi, T., Fukayama, M., Aburatani, H. et al. (2006). Fusion between *CIC* and *DUX4* up-regulates *PEA3* family genes in Ewing-like sarcomas with t(4;19)(q35;q13) translocation. *Hum. Mol. Genet.* **15**, 2125-2137.
Kurada, P. and White, K. (1998). Ras promotes cell survival in *Drosophila* by downregulating *hid* expression. *Cell* **95**, 319-329.
Lam, Y. C., Bowman, A. B., Jafar-Nejad, P., Lim, J., Richman, R., Fryer, J. D., Hyun, E. D., Duvick, L. A., Orr, H. T., Botas, J. et al. (2006). ATAXIN-1 interacts with the repressor Capicua in its native complex to cause SCA1 neuropathology. *Cell* **127**, 1335-1347.
Lee, Y., Fryer, J. D., Kang, H., Crespo-Barreto, J., Bowman, A. B., Gao, Y., Kahle, J. J., Hong, J. S., Kheradmand, F., Orr, H. T. et al. (2011). ATXN1 protein family and CIC regulate extracellular matrix remodeling and lung alveolarization. *Dev. Cell* **21**, 746-757.
Li, B., Gordon, G. M., Du, C. H., Xu, J. and Du, W. (2010). Specific killing of Rb mutant cancer cells by inactivating TSC2. *Cancer Cell* **17**, 469-480.
Marchong, M. N., Yurkowski, C., Ma, C., Spencer, C., Pajovic, S. and Gallie, B. L. (2010). *Cdh11* acts as a tumor suppressor in a murine retinoblastoma model by facilitating tumor cell death. *PLoS Genet.* **6**, e1000923.
Moon, N. S., Frolov, M. V., Kwon, E. J., Di Stefano, L., Dimova, D. K., Morris, E. J., Taylor-Harding, B., White, K. and Dyson, N. J. (2005). *Drosophila* E2F1 has context-specific pro- and antiapoptotic properties during development. *Dev. Cell* **9**, 463-475.
Moon, N. S., Di Stefano, L. and Dyson, N. (2006). A gradient of epidermal growth factor receptor signaling determines the sensitivity of *rbf1* mutant cells to E2F-dependent apoptosis. *Mol. Cell. Biol.* **26**, 7601-7615.
Sherr, C. J. (1996). Cancer cell cycles. *Science* **274**, 1672-1677.
Stevaux, O. and Dyson, N. J. (2002). A revised picture of the E2F transcriptional network and RB function. *Curr. Opin. Cell Biol.* **14**, 684-691.
Tanaka-Matakatsu, M., Xu, J., Cheng, L. and Du, W. (2009). Regulation of apoptosis of *rbf* mutant cells during *Drosophila* development. *Dev. Biol.* **326**, 347-356.
Tseng, A. S., Tapon, N., Kanda, H., Cigizoglu, S., Edelmann, L., Pellock, B., White, K. and Hariharan, I. K. (2007). Capicua regulates cell proliferation downstream of the receptor tyrosine kinase/ras signaling pathway. *Curr. Biol.* **17**, 728-733.
van den Heuvel, S. and Dyson, N. J. (2008). Conserved functions of the pRB and E2F families. *Nat. Rev. Mol. Cell Biol.* **9**, 713-724.
Zhang, J., Benavente, C. A., McEvoy, J., Flores-Otero, J., Ding, L., Chen, X., Ulyanov, A., Wu, G., Wilson, M., Wang, J. et al. (2012). A novel retinoblastoma therapy from genomic and epigenetic analyses. *Nature* **481**, 329-334.